Thin Solid Films 520 (2012) 1705–1708

Contents lists available at SciVerse ScienceDirect

Thin Solid Films

journal homepage: www.elsevier.com/locate/tsf

Growth of single-phase $Mg_{0.3}Zn_{0.7}O$ films suitable for solar-blind optical devices on RS-MgO substrates

H.L. Liang [a], Z.X. Mei [a,*], Z.L. Liu [a], Y. Guo [a], A.Yu. Azarov [b], A.Yu. Kuznetsov [b], A. Hallen [c], X.L. Du [a,**]

[a] Beijing National Laboratory for Condensed Matter Physics, Institute of Physics, Chinese Academy of Sciences, Beijing 100190, China
[b] Department of Physics, University of Oslo, P.O. Box 1048 Blindern, NO-0316 Oslo, Norway
[c] ICT-MAP, Royal Institute of Technology, Electrum 229 SE-164 40, Kista-Stockholm, Sweden

ARTICLE INFO

Article history:
Received 15 November 2010
Received in revised form 24 July 2011
Accepted 7 August 2011
Available online 11 August 2011

Keywords:
Magnesium zinc oxide
Molecular beam epitaxy
Magnesium oxide
Solar-blind
Rutherford backscattering spectrometry
X-ray diffraction

ABSTRACT

Single-phase rock-salt $Mg_{0.3}Zn_{0.7}O$ film was fabricated on MgO (100) substrate by radio-frequency plasma assisted molecular beam epitaxy. A smooth surface was observed by in-situ reflection high-energy electron diffraction and ex-situ atomic force microscopy. X-ray diffraction characterization demonstrated a high-quality single-phase structure with highly (200) orientation and cube-on-cube epitaxial relationship. Zn fraction in the single-phase rock-salt $Mg_{0.3}Zn_{0.7}O$ film was determined by Rutherford backscattering spectrometry. Optical property of the film was investigated by reflectance spectroscopy, which indicated a solar-blind band gap of 255.5 nm. The reason why Zn solubility limit is greatly enhanced in non-polar (100) film compared with (111) polar epilayer is tentatively discussed in this work, suggesting MgO (100) is more suitable for the synthesis of single-phase rock-salt MgZnO with high Zn content towards solar-blind opto-device applications.

1. Introduction

In recent decades, MgZnO, an alloy of wurtzite ZnO (W-ZnO) and rock-salt MgO (RS-MgO), has been attracting more and more attention due to the tunable wide band gap from 3.37 eV (band gap of W-ZnO) to 7.8 eV (band gap of RS-MgO) and large exciton binding energy (60 meV for ZnO and 85 meV for MgO) [1,2]. These superior properties make this material a promising candidate for many potential applications such as ultraviolet (UV) light emitting diodes [3], nonvolatile resistive random access memory devices [4], and short wavelength photo-detectors [5]. Photo-detectors working in short wavelength, especially in the solar-blind UV spectrum region (220–280 nm), have a big advantage of high signal/noise ratio and sensitivity because of the low background radiation at the Earth's surface resulting from the strong atmospheric absorption of sunlight. In this case, a large number of materials have been explored and investigated for the fabrication of solar-blind UV photo-detectors, among which MgZnO is most competitive considering its wide band gap tunability hopefully covering the whole solar-blind range, as well as its nontoxicity and low growth temperature.

However, although the ionic radii of Zn^{2+} and Mg^{2+} are very close to each other [6], phase separation naturally happens due to the large crystal structure dissimilarity between W-ZnO and RS-MgO. So far, the highest Mg content in single wurtzite MgZnO ever reported is 55% [7], which just reached into the solar-blind range from the longer wavelength side. To realize solar-blind photo-detectors working in deeper UV region, i.e. around 260 nm, synthesis of RS-MgZnO with high Zn content is necessary because it can narrower the band gap of RS-MgO and approach the target from the shorter wavelength side [8].

A $Mg_{0.82}Zn_{0.18}O$ component with a band gap of 6.7 eV was prepared on Si (100) by J. Narayan et al. [9], and several attempts in engineering ~50% Zn/Mg content in RS-MgZnO on mismatched c-plane sapphire substrates were also reported [10,11], which may be the highest Zn content in cubic MgZnO grown on sapphire (0001). Few results have been found on homo-epitaxial RS-MgZnO films on RS-MgO substrates, however, except that L. K. Wang et al. reported a cubic $Mg_{0.33}Zn_{0.67}O$ film with an optical band gap of ~250 nm synthesized on MgO (100) by metal organic chemical vapor deposition recently [12].

Our present work contributes to fabricate solar-blind RS-MgZnO homo-epitaxial film by molecular beam epitaxy (MBE) technique. A high-quality single-phase RS-$Mg_{0.3}Zn_{0.7}O$ epilayer was obtained, confirmed by in-situ reflection high-energy electron diffraction (RHEED) observations and ex-situ X-ray diffraction (XRD) characterization. High Zn content of 70% was determined by Rutherford backscattering spectrometry (RBS), resulting in a solar-blind band gap of 4.85 eV (255.5 nm). The reason why Zn solubility limit is greatly enhanced in non-polar (100) film compared with (111) polar epilayer is also tentatively discussed in this work, which indicates that MgO

* Corresponding author. Tel.: +86 10 82648062; fax: +86 10 82649542.
** Corresponding author. Tel.: +86 10 82649035; fax: +86 10 82649542.
E-mail addresses: zxmei@aphy.iphy.ac.cn (Z.X. Mei), xldu@aphy.iphy.ac.cn (X.L. Du).

0040-6090/$ – see front matter © 2011 Elsevier B.V. All rights reserved.
doi:10.1016/j.tsf.2011.08.019

(100) is more suitable for the synthesis of solar-blind RS-MgZnO with high Zn content.

2. Experiments

RS-MgZnO films were synthesized on MgO (100) substrates by radio-frequency plasma assisted MBE (rf-MBE) with a background pressure of ~1×10^{-8} Pa. Elemental Mg (5 N) and Zn (7 N) evaporated by Knudsen cells (CreaTech) and radical oxygen (5.5 N) generated by rf-plasma system (SVTA) were used as sources for the growth. The MgO substrate was degreased in acetone and ethanol before loading into the growth chamber. After that, it was thermally cleaned at 750 °C for 30 min and then exposed to oxygen radicals for 30 min at 650 °C to remove the surface defect layer and contaminations caused by the mechanical polishing process. Further, a thin MgO buffer layer was grown at 500 °C and annealed at 750 °C for 10 min to improve the crystalline quality. Subsequently, MgZnO alloy films were deposited at 350 °C by using a low Zn/Mg flux ratio for the buffer layer and a high Zn/Mg flux ratio for the epilayer, respectively. The film thickness is around 350 nm.

RHEED technique was applied to in-situ monitor the whole growth process and the crystal phase evolutions. Surface morphology and roughness of the film was evaluated by using commercial atomic force microscopy (AFM, SPA-400, SIINT) with contact mode tips (OMCL-TR400PSA, Olympus). The crystal structure of the film was further investigated by XRD technique (M18AHF, Mac Science) with regular Cu K_α radiation as well as high-resolution XRD using light source from synchrotron radiation. The composition was confirmed by RBS employing 2 MeV He^+ ions and SIMNRA code [13] for fitting the experimental and simulation data. Reflectance spectroscopy with an integration step of 0.5 nm was performed on a commercial spectrophotometer system (Lambda 950, Perkin Elmer) to determine the band gap energy.

3. Results and Discussion

RHEED was firstly adopted to monitor the whole growth process and phase evolutions. Before MgZnO deposition, a high-quality cubic-MgO (100) template was obtained with a flat surface, which is indicated by the well-defined patterns and streaky Kichuchi lines [Fig. 1 (a)]. Fig. 1 (b) illustrates a typical single-phase RS-MgZnO epilayer, having a diffraction pattern very similar to that of cubic-MgO template with a 4-fold symmetry [Fig. 1 (a)]. A smooth surface is revealed by the sharp contrast and streaky RHEED patterns in Fig. 1 (b).

The surface morphology was evaluated by AFM as shown in Fig. 1 (c). The root mean square roughness of the film in a 5×5 μm^2 scanning area is about 1.56 nm, demonstrating high crystal quality and smooth surface, which is coincident with the in-situ RHEED observations. Besides, as seen in Fig. 1 (c), a cube-like grain can be discerned obviously in a 1×1 μm^2 area, implying a cube-on-cube epitaxial relationship between the epilayer and the substrate.

Further, Fig. 2 (a) shows XRD θ-2θ scan of the sample. Only two diffraction peaks were detected in the scanning range of 30°–45°, 42.08° and 42.9°, respectively. The peak located at 42.08° is attributed to the diffraction from RS-MgZnO (200) planes, and 42.9° from RS-MgO (200) planes. Importantly, the appearance of only (200) related peak combined with the RHEED findings proves the single crystalline rock-salt structure of the film. The rocking curve of RS-MgZnO (002) plane was performed using the light source from synchrotron radiation (not shown here). Three Gaussian peaks, corresponding to the substrate, the buffer layer and the epilayer, were used to fit the obtained curve. The FWHM values of the three layers are 0.06°, 0.24° and 0.48°, respectively, demonstrating a highly aligned orientation parallel to the growth plane. Further increase of Zn/Mg flux ratio will result in the formation of W-MgZnO in RS matrix, as confirmed by the appearance of secondary diffraction peak from W-MgZnO (002) planes located around 34.47°, as well as the evolution of new patterns from wurtzite phase in RHEED observations (not shown here).

In addition, Fig. 2 (b) shows the ϕ-scan result of MgZnO (111) plane which was carried out at around $\chi = 54.7°$ (the angle between (100) and (111) planes in a cubic system). Four sharp peaks with 90°apart can be seen clearly, indicating a 4-fold symmetry for the RS-MgZnO film with (200) orientation, which agrees well with the in-situ RHEED observations.

Fig. 3 shows the corresponding RBS spectra taken from the single-phase cubic MgZnO sample. Arrows/labels in Fig. 3 indicate the channel numbers at which the backscattering from corresponding elements starts. The fitting of the experimental and simulation data in Fig. 3 reveals the Zn composition in the epilayer is 70%.

In accordance with the method suggested previously to investigate band gap variations in AlGaN alloys [13], room-temperature reflectance spectroscopy was applied to determine the band gap of the cubic $Mg_{0.3}Zn_{0.7}O$ sample and Fig. 4 shows the result of the measurement. It exhibits a sharp characteristic peak corresponding to the band gap energy [indicated by a black arrow], followed by typical Fabry-Perot oscillations. The band gap is determined as 4.85 eV (255.5 nm), which is within the solar-blind range, offering promising applications of our material as solar-blind UV detecting components.

All above-mentioned results demonstrate a single-phase RS-MgZnO fabricated on MgO (100) substrates with much higher Zn content than those on MgO (111) templates [14]. The same phenomenon was observed in homo-epitaxial $GaAs_{1-x}N_x$ growth on

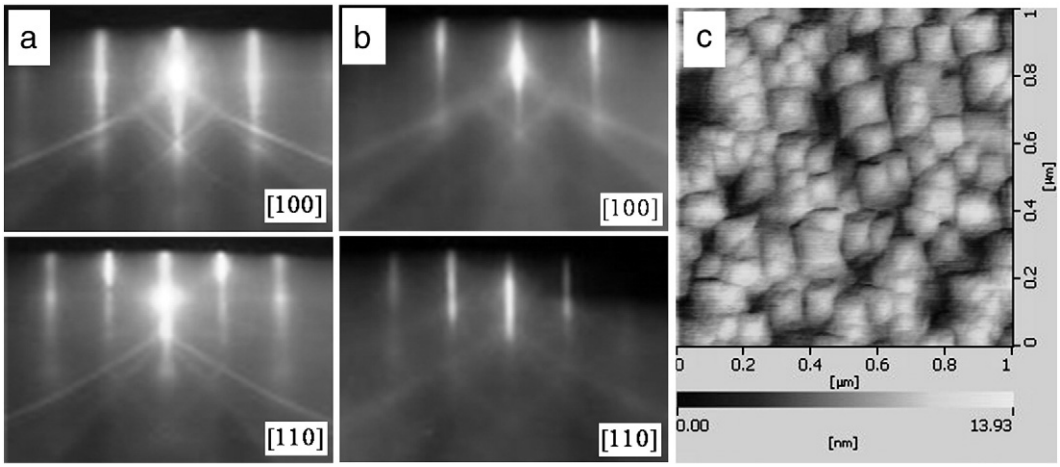

Fig. 1. RHEED patterns along two fixed electron azimuths directions as recorded at different stages in sample synthesis: (a) cubic-MgO (100) buffer, (b) RS-$Mg_{0.3}Zn_{0.7}O$ epilayer demonstrating single phase, and (c) AFM image of the RS-$Mg_{0.3}Zn_{0.7}O$ epilayer in a 1×1 μm^2 scanning area.

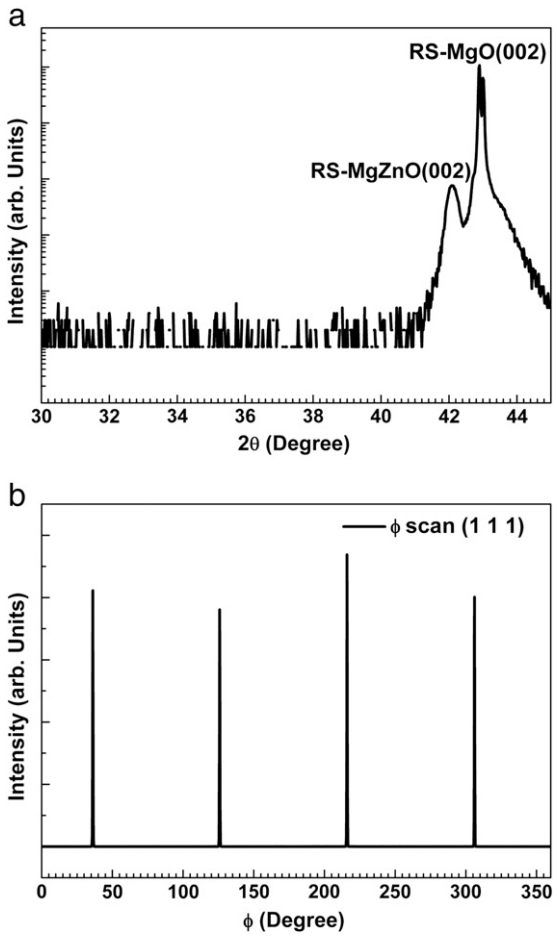

Fig. 2. (a) XRD θ-2θ scan of RS-$Mg_{0.3}Zn_{0.7}O$ (100) plane, and (b) XRD ϕ-scan of RS-$Mg_{0.3}Zn_{0.7}O$ (111) plane.

GaAs substrates with different orientations [15]. The reason why MgO (100) is better for the increasing of Zn solubility is supposed as follows. MgO (111) plane is a polar surface and its in-plane atom configuration is obviously different from that of MgO (100) which is non-polar surface [16]. As shown in Fig. 5, (100) has Mg and O atoms alternately, but (111) only one kind of atom, Mg or O. When the growth starts, the atoms coming to MgO (111) surface will be stacking in the way of one single polar ion layer above another, that is, anion (oxygen) layer and cation (both Mg and Zn) layer in turn. At first, Zn–

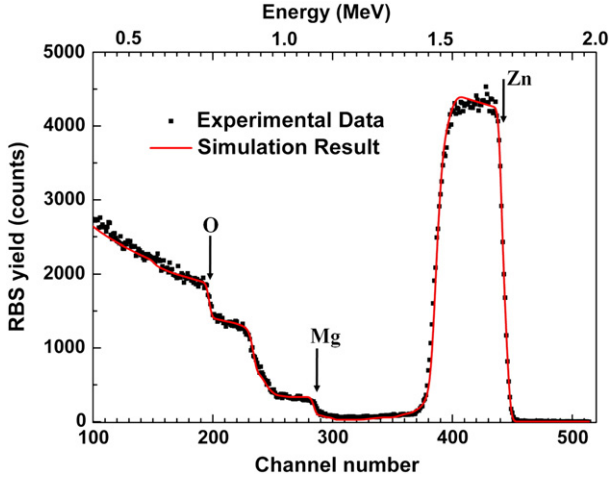

Fig. 3. RBS spectra (points) and the corresponding best-fit simulation (line).

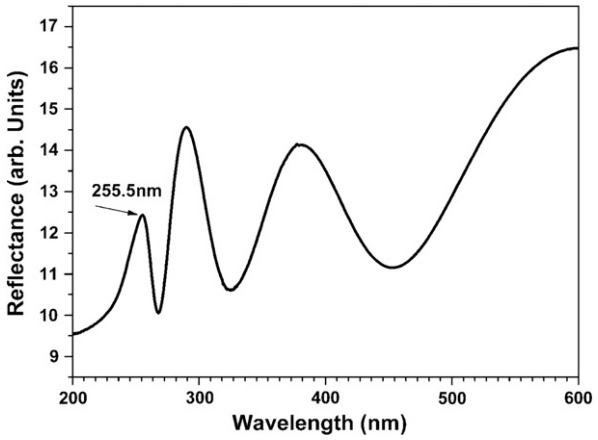

Fig. 4. Reflectance spectra measured at room temperature. The black arrow indicates the band gap position of the sample.

O bond is the same as Mg–O bond with a coordination number of 6 due to the strong confinement effect of the substrate. However, as the film thickness increases, influence from the substrate becomes weaker and weaker, and the lattice strain becomes dominant. The high surface free energy of (111) polar plane plays an important role in deciding the film structures then. When Zn content exceeds the non-equilibrium solubility limit, 50% or so, Zn-O bond cannot hold the RS coordination and will relax into the thermal-equilibrium sp^3 hybrid coordination in wurtzite structure, resulting in wurtzite and cubic phase separation. On the contrary, Mg, Zn, and O atoms coming to MgO (100) surface will be bonded to each other in one single layer. The surface free energy of this non-polar surface is not as high as that of (111) polar surface. In this case, it is much easier for Zn–O bond to keep 6 coordination and maintain the RS structure with Mg-O bond together. As a result, Zn content can reach as high as 70% before phase separation happens. Therefore, MgO (100) is more suitable for the synthesis of single-phase RS-MgZnO with high Zn content towards solar-blind opto-device applications.

4. Conclusions

In summary, synthesis of single-phase RS-MgZnO on MgO (100) substrate by rf-plasma assisted MBE was investigated. It is found that MgO (100) is a favorable substrate for the growth of high Zn content cubic MgZnO films. The in-situ RHEED observations combined with ex-situ AFM and XRD characterizations demonstrate the high crystal quality and smooth surface with a cube-on-cube epitaxial relationship. Band gap of the single-phase RS-$Mg_{0.3}Zn_{0.7}O$ film is determined as 255.5 nm, showing the prospects in solar-blind UV detector applications.

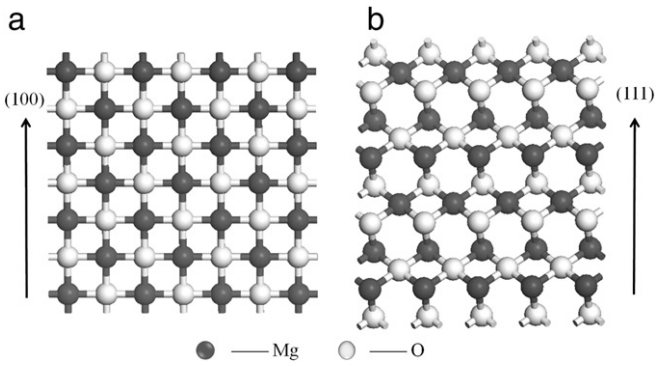

Fig. 5. The cross-sectional atomic arrangements along the growth direction corresponding to (a) MgO (100) and (b) MgO (111).

Acknowledgments

This work was supported by the National Science Foundation (Grant nos. 61076007, 50532090, and 60606023), the Ministry of Science and Technology (Grant nos. 2007CB936203, 2009CB929400, 2009AA033101 and 2011CB302002) of China, the Chinese Academy of Sciences, the Diffusion Scattering Station in Beijing Synchrotron Radiation Facility, as well as the Research Council of Norway through the FRINAT "Understanding ZnO" project.

References

[1] A. Ohtomo, M. Kawasaki, T. Koida, K. Masubuchi, H. Koinuma, Y. Sakurai, Y. Yoshida, T. Yasuda, Y. Segawa, Appl. Phys. Lett. 72 (1998) 2466.
[2] R.C. Whited, W.C. Walker, Phys. Rev. Lett. 22 (1969) 1428.
[3] A. Tsukazaki, A. Ohtomo, T. Onuma, M. Ohtani, T. Makino, M. Sumiya, K. Ohtani, S. Chichibu, S. Fuke, Y. Segawa, H. Ohno, H. Koinuma, M. Kawasaki, Nat. Mater. 4 (2005) 42.
[4] X.M. Chen, G.H. Wu, D.H. Bao, Appl. Phys. Lett. 93 (2008) 093501.
[5] T. Tut, M. Gokkavas, A. Inal, E. Ozbay, Appl. Phys. Lett. 90 (2007) 163506.
[6] R.D. Shannon, Acta Cryst. A32 (1976) 751.
[7] Z.L. Liu, Z.X. Mei, T.C. Zhang, Y.P. Liu, Y. Guo, X.L. Du, A. Hallen, J.J. Zhu, A.Yu. Kuznetsov, J. Cryst. Growth 311 (2009) 4356.
[8] W. Yang, S.S. Hullavarad, B. Nagaraj, I. Takeuchi, R.P. Sharma, T. Venkatesan, R.D. Vispute, H. Shen, Appl. Phys. Lett. 82 (2003) 3424.
[9] J. Narayan, A.K. Sharma, A. Kvit, C. Jin, J.F. Muth, O.W. Holland, Solid State Commun. 121 (2002) 9.
[10] S. Choopun, R.D. Vispute, W. Yang, R.P. Sharma, T. Venkatesan, H. Shen, Appl. Phys. Lett. 80 (2002) 1529.
[11] Z.G. Ju, C.X. Shan, D.Y. Jiang, J.Y. Zhang, B. Yao, D.X. Zhao, D.Z. Shen, X.W. Fan, Appl. Phys. Lett. 93 (2008) 173505.
[12] L.K. Wang, Z.G. Ju, C.X. Shan, J. Zheng, B.H. Li, Z.Z. Zhang, B. Yao, D.X. Zhao, D.Z. Shen, J.Y. Zhang, J. Cryst. Growth 312 (2010) 875.
[13] L.S. Yu, D. Qiao, S.S. Lau, J.M. Redwing, Appl. Phys. Lett. 75 (1999) 1419.
[14] H.L. Liang, Z.X. Mei, Z.L. Ziu, Y. Guo, A.Yu. Azarov, A.Yu. Kuznetsov, A. Hallen, X.L. Du, AIP Conf. Proc. 1292 (2010) 185.
[15] A. Arnoult, F. Gonzalez-Posada, S. Blanc, V. Bardinal, C. Fontaine, Phys. E 23 (2004) 352.
[16] S. Han, D.Z. Shen, J.Y. Zhang, Y.M. Zhao, D.Y. Jiang, Z.G. Ju, D.X. Zhao, B. Yao, J. Alloys Compd. 485 (2009) 794.